Hybrid Smart Antenna System Using Directional Elements—Performance Analysis in Flat Rayleigh Fading

Zhijun Zhang, *Member, IEEE*, Magdy F. Iskander, *Fellow, IEEE*, Zhengqing Yun, *Member, IEEE*, and Anders Høst-Madsen, *Senior Member, IEEE*

***Abstract*—Smart antenna and associated technologies are expected to play a significant role in enabling broadband wireless communication systems. Smart antennas exploit space diversity to help provide high data rates, increased channel capacity, and improved quality of service at an affordable cost. In this paper we present a new procedure for implementing smart antenna algorithms. It is a hybrid approach that integrates the features of the switched beam method and the adaptive beam forming approach. Specifically it is shown that by using high gain antenna elements and combining the switched beam process with the adaptive beam forming procedure on a limited number of elements (as low as two in an eight-element array), a performance close to that of a more complex eight-element adaptive array may be achieved. The proposed hybrid method, therefore, is fast, is computationally efficient, and provides a cost effective approach for exploiting space diversity. Even with the inclusion of interference signals, the proposed hybrid approach out-performed the switched beam method, and provided performance similar to that of an adaptive array with less number of elements (three in an eight-element array). Implementation of an adaptive array also includes estimations; hence, reducing the number of elements in an array may lead to improved accuracy, in addition to fast convergence and reduced complexity.**

***Index Terms*—Adaptive array, hybrid smart antenna, Rayleigh fading, smart antenna, switched beam.**

I. Introduction

THE DEMAND for increased capacity in wireless communications networks has motivated recent research activities toward wireless systems that exploit the concept of smart antenna and space selectivity. The deployment of smart antennas at existing cellular base station installations has gained enormous interest because it has the potential to increase cellular system capacity, extend radio coverage, and improve quality of services [1]–[12]. Smart antennas may be used to provide significant advantages and improved performance in almost all wireless communication systems, including time-division multiple-access (TDMA) cellular systems, code-division multiple-access (CDMA) cellular systems [4], as well as others.

One smart antenna implementation strategy uses an adaptive antenna array, whose outputs are adaptively combined through a set of complex weights (signal amplitude and phase adjustments) to form a single output with beam steering and interference mitigation capabilities. Signal processing aspects for this type of systems have concentrated on the development of efficient algorithms for direction of arrival (DOA) estimation [5] and adaptive beamforming. Algorithms for adaptive beamforming have departed from the classical least mean square (LMS) type algorithm [6] to more sophisticated constant modulus algorithm (CMA) [7] and the eigen-projection algorithms [8]. Other issues that have been examined include analyzing the effects of mutual coupling between the array elements [9] on adaptive algorithms and combating the effects of fading channels on the overall system [10]. Directional elements were used in the adaptive smart antenna design [11], but specific results regarding achieved improvement were not reported.

Another smart antenna implementation strategy uses a switched-beam antenna array consisting of multiple narrow-beam directional antennas, along with a beam-selection algorithm. The selection of the activated receive beam is based on the received signal-strength. The same beam is used for both reception and transmission. Beam forming is accomplished by using physically directive antenna elements to create aperture efficiency and gain [2], [3]. If the received carrier to interference ratio (CIR) falls below some preset level during a call, the base station then switches to the best available beam for transmission and reception.

In comparing the above two implementation procedures, it may be noted that adaptive implementations have better performance than switched-beam implementations. This comes at the expense of relatively higher implementation cost and complexity constraints, as compared with the switched-beam implementation procedure. Furthermore, adaptive algorithms rely on estimations and this may contribute to slow convergence, compromise accuracy, and generally, lead to less than optimal performance.

Dense scattering and cluster angle distribution phenomena of a multipath environment [13], [14] are well known and are expected to impact the performance of a smart antenna system. It would be helpful if a procedure could be developed that will help evaluate the impact of the propagation environment on the system performance and provide specific smart antenna designs for different propagation environments. It would also be desirable to develop a smart antenna system with sufficient flexibility in the design arrangements so as to meet varying conditions in the propagation environments. It is the objective of this paper to describe the development of a smart antenna system that provides considerable design flexibility to meet changes in prop-

Manuscript received August 7, 2002; revised November 8, 2002.

The authors are with the Hawaii Center for Advanced Communications, College of Engineering, University of Hawaii at Manoa, Honolulu, HI 96822 USA.

Digital Object Identifier 10.1109/TAP.2003.818002

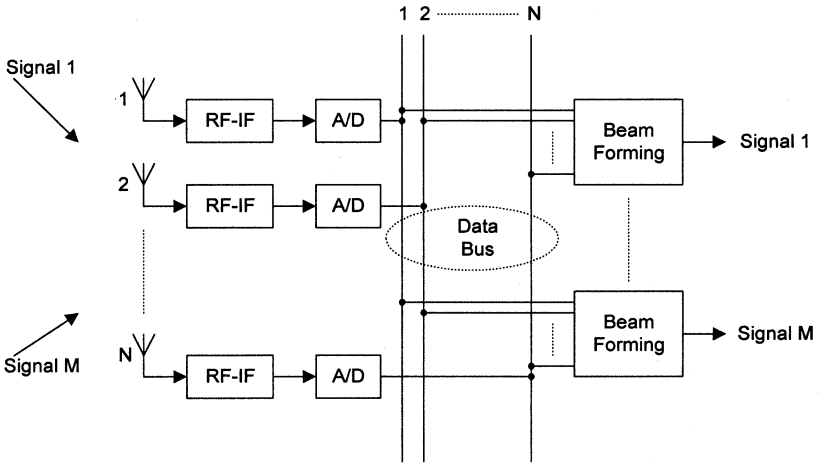

Fig. 1. Adaptive smart antenna system diagram.

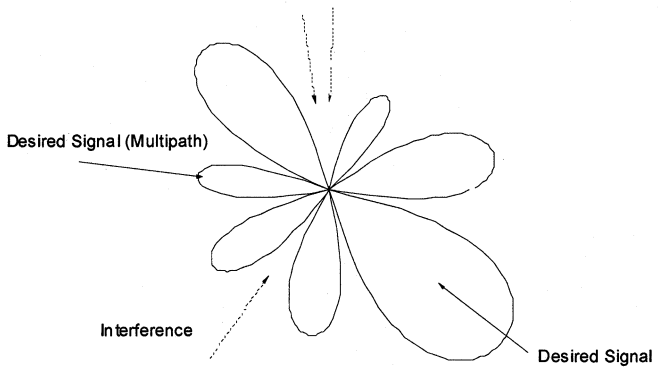

Fig. 2. Adaptive pattern of one beam-forming block. Desired signals and interferences are denoted by solid arrows and dashed arrows, respectively.

agation environment. Accounting for specific and varying aspects of the propagation environment will be discussed in a future paper.

II. Hybrid Smart Antenna System

Fig. 1 shows an N element adaptive smart antenna receiver system. Let us assume that the system is required to support M users. For a signal from any user, due to a multipath environment and the different positions of the antennas, there will be phase and amplitude differences in the signals received by the N antenna elements. The output signal from any element is a particular combination of all M signals and their multipath signals. These signals will first go through RF to IF blocks, and then they will be converted to a digital stream by analog-to-digital converters and sent to the data bus. There are M beam-forming blocks connected to the data bus. Each of these blocks needs to process N digital streams obtained from the data bus, and generate a pattern to receive the signal from one of the M users.

Fig. 2 shows a pattern formed by a beam-forming block shown in Fig. 1. Multipath signals and undesired interferences are noted by solid-arrow lines and dash-arrow lines, respectively. As may be seen, an adaptive implementation can dynamically point pattern peaks to desired and multipath signals, and adjust the nulls to cancel unwanted interferences. With the increase in the number of total antenna elements, the system complexity increases significantly.

Fig. 3 shows a switched-beam smart antenna system formed by N directional antenna elements. Each antenna covers an angle range of $360^\circ/N$. As shown in Fig. 4, the system can automatically switch to an antenna that has its main beam in the domain of the desired signal. Because the preformed pattern has a narrow main beam, most multipath and interference signals will fall into the side lobe range, resulting in suppression of these signals and improved system performance. Comparing this with the adaptive implementation, it may be noted from Fig. 4 that the switched-beam method cannot make full use of the multipath signals, and cannot be used to cancel interferences when located in the main lobe. Thus, the performance of a switched-beam system is less optimal when compared with an adaptive system. This will also be confirmed in Section IV by simulation of several representative cases.

Fig. 5 shows a proposed alternative hybrid smart antenna system. The proposed system described in this paper combines the advantages of both switched-beam and adaptive systems. Unlike traditional adaptive antenna arrays, the proposed system uses directional elements to achieve additional antenna gain. It does have beamforming capabilities to cancel interferences but uses a smaller number of signals than traditional adaptive systems. Through the proper design of the proposed system, it may be expected that it is possible to achieve a performance similar to that of an adaptive system with the advantage of using a lesser number of signals in the adaptive process. Similar to the traditional switched beam array process, signal selection will be based on combining the strongest signals in the overall array.

As shown in Fig. 5, the proposed system inherits part of the characteristics of the switched-beam system, in that it adopts directional antenna elements. It will be described in Section IV that different coverage angles should be chosen in different multipath scenarios to obtain the best performance. The arrangement in Fig. 5 also borrows some digital beamforming technology used in adaptive systems, but in this case the beamforming will be done more efficiently using a reduced number of signals. There are additional blocks (N to NS selector) that select only the NS ($NS < N$) strongest signal streams from total

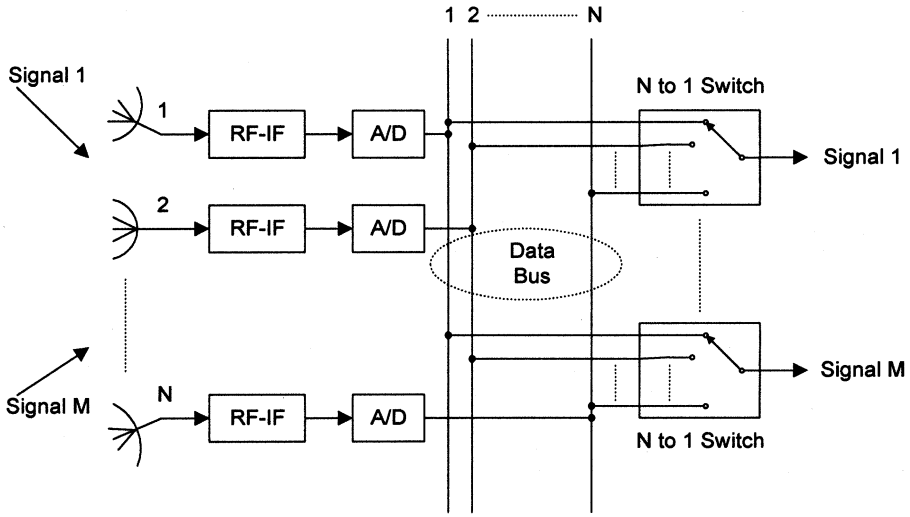

Fig. 3. Switched-beam smart antenna system diagram.

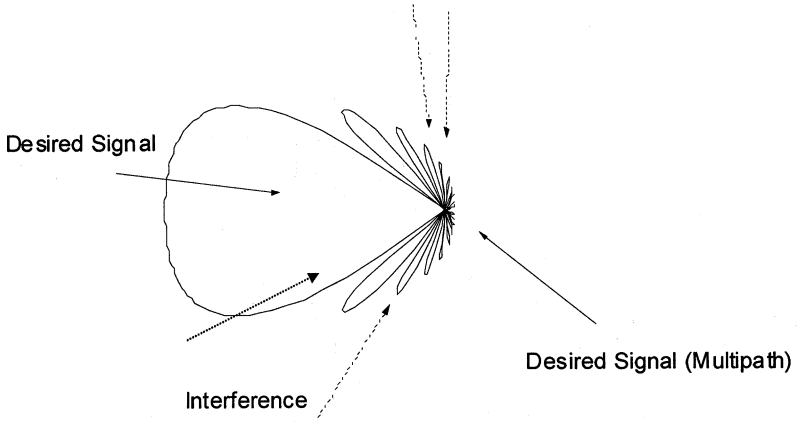

Fig. 4. Pattern of switched-beam smart antenna. Desired signals and interferences denoted by solid and dashed arrows, respectively.

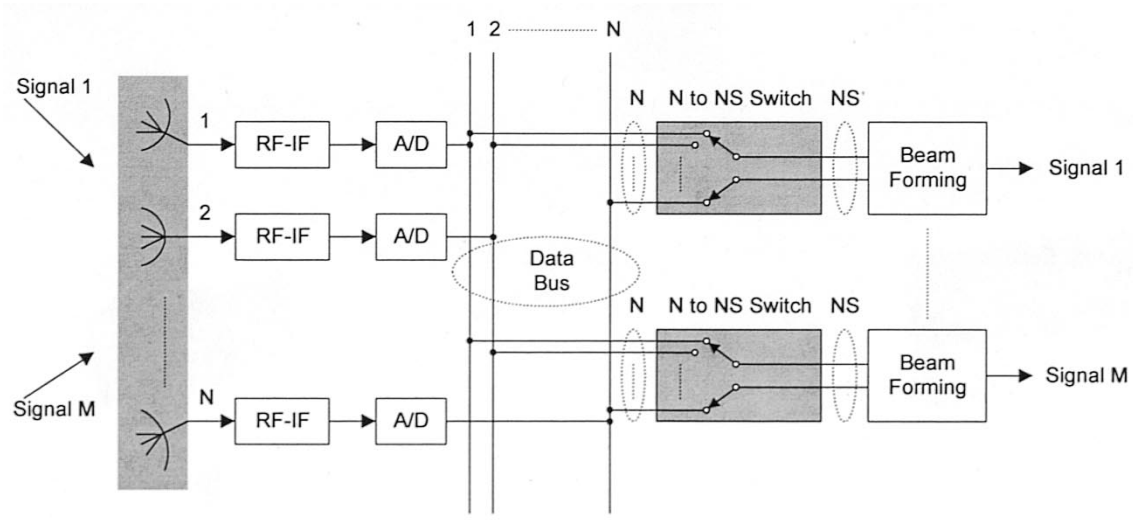

Fig. 5. Proposed hybrid smart antenna system. N antenna elements are used to receive M signals. The beam-forming process is performed on a smaller number ($NS < N$) of signals.

N streams on the data bus. Considering the slow angle movement of mobile users and the relatively wide beamwidth of the radiation pattern of antenna elements, the N to NS switches do not need to be updated in real time. It will be shown that in most cases when using the arrangement in Fig. 5, performance similar to that of an eight-element adaptive system can be achieved

by using a value of NS as small as 2. It will also be shown that as NS increases, the performance will continue to improve; but the system complexities will also increase and ultimately converge to a fully adaptive antenna array.

III. Assumptions and Description of the Simulation Model

Fig. 6 shows a block diagram of an N-element beam forming smart antenna system. The baseband signal $x(t)$ received by the antenna array is given by

$$\boldsymbol{x}(t) = \mathbf{U}^d \boldsymbol{s}^d + \mathbf{U}^i \boldsymbol{s}^i + \boldsymbol{n} \tag{1}$$

where $\mathbf{U}^d$ and $\mathbf{U}^i$ are matrices of the channel transfer functions of the multipath signal and interferences, respectively. $\boldsymbol{s}^d$ and $\boldsymbol{s}^i$ are vectors of the multipath signals and interferences, respectively. $\boldsymbol{n}$ is the system noise. The channel transfer functions and the signal vectors are given by

$$\boldsymbol{x}(t) = (x_1(t), x_2(t), \ldots, x_N(t))^T \tag{2}$$

$$\mathbf{U}^d = \begin{pmatrix} u^d_{1,1} & \cdots & u^d_{1,P} \\ \vdots & u^d_{n,p} & \ddots \\ u^d_{N,1} & \ddots & u^d_{N,P} \end{pmatrix}_{N*P} \bullet \begin{pmatrix} f_1(\theta^d_1) & \cdots & f(\theta^d_P) \\ \vdots & f_n(\theta^d_p) & \ddots \\ f_N(\theta^d_1) & \ddots & f_N(\theta^d_P) \end{pmatrix}_{N*P} \tag{3}$$

$$\mathbf{U}^i = \begin{pmatrix} u^i_{1,1} & \cdots & u^i_{1,I} \\ \vdots & u^i_{n,i} & \ddots \\ u^i_{N,1} & \ddots & u^i_{N,I} \end{pmatrix}_{N*I} \bullet \begin{pmatrix} f_1(\theta^i_1) & \cdots & f(\theta^i_I) \\ \vdots & f_n(\theta^i_i) & \ddots \\ f_N(\theta^i_1) & \ddots & f_N(\theta^i_I) \end{pmatrix}_{N*I} \tag{4}$$

$$\boldsymbol{s}^d = \left(s^d_1(t), \ldots, s^d_p(t), \ldots, s^d_P(t)\right)^T \tag{5}$$

$$\boldsymbol{s}^i = \left(s^i_1(t), \ldots, s^i_i(t), \ldots, s^i_I(t)\right)^T \tag{6}$$

$$\boldsymbol{n} = (n_1, n_2, \ldots, n_N)^T \tag{7}$$

where operator ($\bullet$) indicates the dot product. The element $u^d_{n,p}$ in the multipath channel transfer function represents the propagation transfer function of the pth multipath signal to the nth antenna. The matrix element $u^i_{n,i}$, on the other hand, represents the propagation transfer function of the ith interference to the nth antenna. Both $u^d_{n,p}$ and $u^i_{n,i}$ are complex Gaussian random variables. The function $f_n(\cdot)$ describes the antenna amplitude pattern of the nth antenna element. θ^d_p is the angle of arrival of the pth multipath of the desired signal and θ^i_i is the angle of arrival of the ith interference. $s^d_p(t)$ is the pth multipath of the desired signal. $s^i_i(t)$ is the ith interference. n_n is the noise at the nth antenna, and is modeled as a stationary, complex, Gaussian process of zero mean and specially white in the processed frequency band. Without loss of generality, all powers were normalized to noise variance. Thus, n_n has complex Gaussian distribution $CN(0, 1)$; $u^d_{n,p}$ and $u^i_{n,i}$ also have complex Gaussian distribution $CN(0, 1)$.

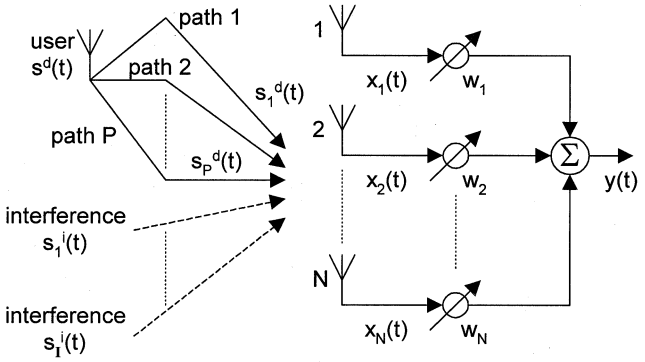

Fig. 6. Block diagram of an N-element beam forming smart antenna system.

The expected input signal-to-noise ratio (SNR) for the desired signal Γ_s and the expected input interference-to-noise ratio (INR) for the ith interference Γ_i are given by

$$\Gamma_s = E\left(\left(s^d\right)^H s^d\right) \tag{8}$$

$$\Gamma_i = E\left(\left(s^i_i\right)^* s^i_i\right). \tag{9}$$

Operator $(*)$ denotes complex conjugate and H denotes complex conjugate transpose. For omni-directional antenna elements, $(f_n(\cdot) = 1)$, the received signal at any antenna element will be the sum of identically distributed Gaussian signals. The magnitude of the received signal will thus have a Rayleigh distribution. A Rayleigh channel corresponds to a multipath environment where all the arrived signals are multipath signals and where there is no-line-of sight propagation path for the desired signal. When there is a line-of-sight signal, the channel should be modeled as a Rician Channel.

The interference-plus-noise covariance matrix [15] is given by

$$\mathbf{R} = \mathbf{U}^i \left(\mathbf{U}^i\right)^H + \mathbf{I}_{N*N} \tag{10}$$

where $\mathbf{I}$ is an identity matrix. Assuming all propagation vectors are known, the optimum-combining weights of an adaptive antenna array that will result in interference cancellation is given by

$$w = \left(\sum_{p=1}^{P} \mathbf{U}^d_{N*1,\,p}\right)^H \mathbf{R}^{-1}. \tag{11}$$

The optimum-combining output in this case will be given by

$$y(t) = \boldsymbol{w}\boldsymbol{x}(t). \tag{12}$$

For performance simulations of a traditional adaptive array, the distance between adjacent elements is assumed to be a half wavelength and each antenna is assumed to be omni-directional as shown in Fig. 7. As may be seen in Fig. 8, the distance between adjacent elements of a hybrid smart antenna array is also assumed to be a half wavelength; but, in this case, each element is assumed to have its own directional pattern.

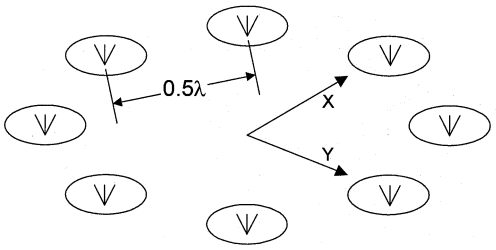

Fig. 7. Planar (x, y) layout of a traditional adaptive smart antenna array consisting of omni-directional elements.

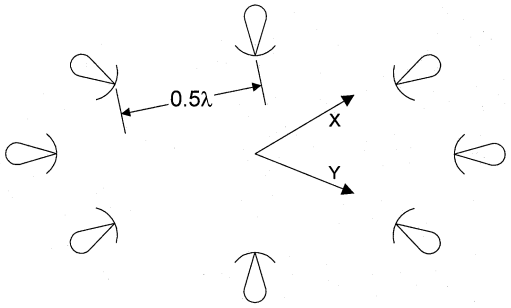

Fig. 8. Planar layout of a hybrid smart antenna array consisting of directional elements.

Fig. 9 shows the pattern used in the simulation of the proposed hybrid smart antenna system. The pattern has a main beam with a ϕ-degree beamwidth. Neglecting the side lobe power, the power gain of the main beam may be approximately estimated as 360° divided by ϕ. The pattern has a -20 dB sidelobe and it should be noted that the initial simulation results showed no observable difference in the system performance results when the sidelobe level was varied by as much as ± 10 dB from the utilized -20 dB value. For the case of an eight-element array with ϕ equal to 45°, the main beam of all the elements will be placed side-by-side to provide the 360° coverage. If ϕ is less than 45° there will be gaps that cannot be covered by the collective main beams of the eight-element array, and if ϕ is larger than 45° there will be an overlap between the patterns from the various antenna elements. One thing that needs to be mentioned is that $f_n(\cdot)$ in (3) and (4) is the amplitude pattern instead of the power pattern, hence a square root operator is needed to get $f_n(\cdot)$ from the power pattern normally measured in antenna characterization.

Two kinds of communication systems, TDMA and CDMA, were simulated in this paper. For a TDMA system, smart antennas are only used to overcome multipath fading and no co-channel interference is assumed. For a CDMA system, all users share the same frequency and channels are distinguished by different codes. Each user thus interferes with other users who are occupying the same frequency band. In a CDMA system; therefore, a smart antenna is used to overcome both multipath fading and interference.

Binary phase shift keying (BPSK) modulation is used in all simulations; therefore, the output of an optimum combining in (12) can be simplified to $\mathrm{Re}(y(t))$. Also, 500 000 random cases were simulated for each SNR value and for each operating case of the proposed antenna structure.

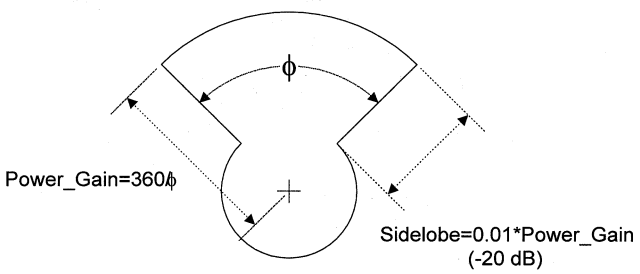

Fig. 9. Antenna pattern used for the hybrid smart antenna simulations.

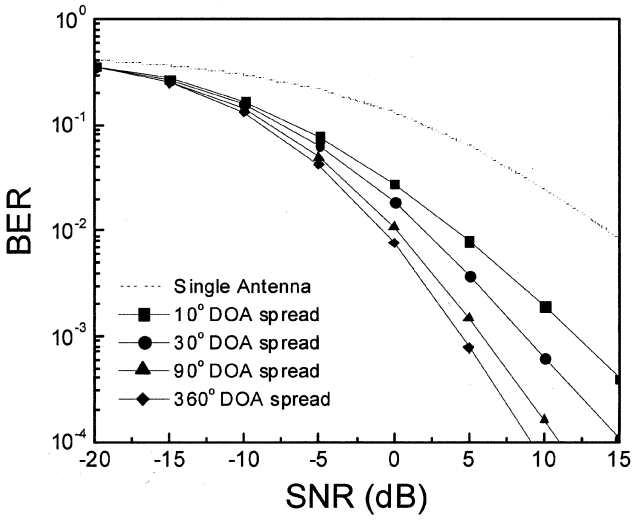

Fig. 10. DOA spread versus Smart antenna performance. Simulation assumes no interference, optimum combining, an eight-element array and five multipath signals.

IV. Simulation Results

Figs. 10–19 show the simulation results for a TDMA communications system. As mentioned earlier, this means that the smart antenna array will be concerned only with the multipath effect and no interference consideration will be included. Figs. 20 and 21 are simulation results for a spread-spectrum system, thus simulation results will include both multipath and inference signals. The following is a detailed discussion of these results.

Fig. 10 and 11 provide reference data on the performance of a traditional adaptive array. When integrating an adaptive smart antenna simulation with a propagation model, there are many different parameters, such as array type, multipath angle spread, delay spread, cluster behavior, etc. that need to be considered. Three variables are inspected in this paper. The first is the number of elements in the array. As expected, more elements improve the system performance; but also increase the system complexity. Eight-element arrays are widely used and are considered as a good tradeoff between performance and complexity. Hence, in all the simulations reported in this paper, we will use eight-element arrays. The second and third variables are all related to the propagation models. One is the DOA spread of a multipath signal and the other is the number of multipath signals. The impact of each of these parameters on the overall system performance was simulated. The following represents samples of the obtained results.

Fig. 10 shows how the performance of an adaptive system is related to the DOA spread of multipath signals. The smart

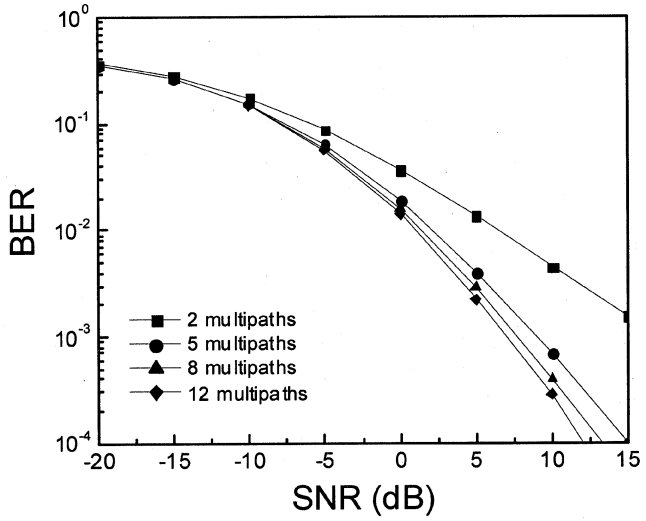

Fig. 11. Multipath number versus Smart antenna performance. Simulation assumes no interference, optimum combining, an eight-element array and 30° DOA spread.

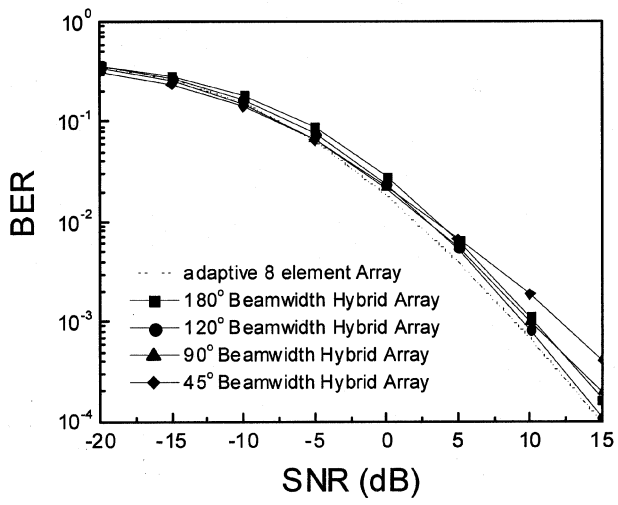

Fig. 12. Performance of a hybrid smart antenna system as a function of the beamwidth of the directional elements. Simulation assumes no interference and that the hybrid array selects and combines two signals from an array of eight elements of directional antennas. 30° DOA spread was assumed.

antenna used in this simulation is a traditional optimum-combining adaptive array with eight omni-directional elements. It was assumed that there were five Gaussian multipath signals. The X axis is the SNR at each antenna element and the Y axis is the bit error rate (BER) of coherent demodulation of BPSK at the array output. It is clear that when the DOA spread of multipath signals decreases from 360° to 10°, the system performance decreases and the SNR required for keeping BER less than 10^{-3} has to increase by 7.8 dB, from 4.4 to 12.2 dB. The BER result of a single antenna is also shown as reference by the dotted line in the same figure. This can be explained in terms of the fact that when DOA decreases, multipath signals become more correlated; and hence, cause a decrease in the adaptive array performance.

Fig. 11 shows the impact of the number of multipath on the performance of an adaptive antenna system. The simulated system is also a traditional optimum-combining array with 8 omni-directional elements, and the multipath DOA spread was selected in this case to be 30°. Results in Fig. 11 show that as the number of multipath increases from 2 to 12, the system performance increases and the SNR required for keeping BER less than 10^{-3} is decreased from 17.1 to 6.9 dB. This improved performance can be explained in terms of the reduced correlation of the signals at each antenna due to the richer multipath environment.

For the proposed hybrid smart antenna system, there are five variables that need to be inspected in the simulations. Besides the three variables mentioned above (number of elements, number of multipath, and DOA spread) which are shared with an adaptive smart antenna system, there are two more variables that need to be considered in this case. These include beamwidth of the directional antenna element and the number of elements that will be chosen for the beamforming process (NS in Fig. 5). Simulation results show that the first three variables have similar impact on the performance of the proposed hybrid smart antenna design when compared with the adaptive smart antenna system described above. Thus, only the effect of the last two parameters will be presented and discussed here.

The propagation model used in the simulations in both Figs. 12 and 13 includes five multipath signals with 30° DOA spread. This 30° DOA spread corresponds to a propagation scenario for a base station that is installed on top of a building roof where the use is at a moderate distance from the base station. It is assumed that there are no obstacles around the base station antenna and all multipath signals are caused by cluster reflections around the user.

Fig. 12 inspects how a different antenna beamwidth φ impacts the performance of the proposed hybrid smart antenna system. A different beamwidth also means a different gain because the element gain is assumed to be $360/\varphi$ (see Fig. 9 and neglecting the side lobe power). The hybrid smart antenna used in this simulation selects and combines the two largest signals ($NS = 2$) out of the available ones from the array of eight elements. The dotted line in Fig. 12 shows the results of a traditional adaptive smart antenna method (optimum-combining eight elements) and is included here for reference.

From Fig. 12, it is interesting to note that the 120° beamwidth hybrid array has the best performance, more specifically, that the required SNR to keep BER less than 10^{-3} is only 0.67 dB higher than that for a traditional adaptive antenna system.

Results in Fig. 13 confirm the expected performance and show an improved BER with the increase in the number of elements used in the adaptive process. It may also be noted that results for more than two elements in the proposed hybrid smart antenna array system superpose those for the traditional adaptive array; hence, the increase in the number of signals is unnecessary and just adds to the complexity of the system.

As discussed earlier, a hybrid system takes advantage of both the antenna gain and optimum combining to improve the overall system performance. Fig. 14 shows a case where a 90° beamwidth system is used in a 30° DOA spread environment. Different amplitudes were only used to clarify the graphical illustration. All three antennas were assumed to have the same gain. In Fig. 14 the second antenna can receive all multipath signals, but the first and third antennas can only receive part of these multipath signals. The requirement for an optimum-combining array is that each antenna can receive all multipath

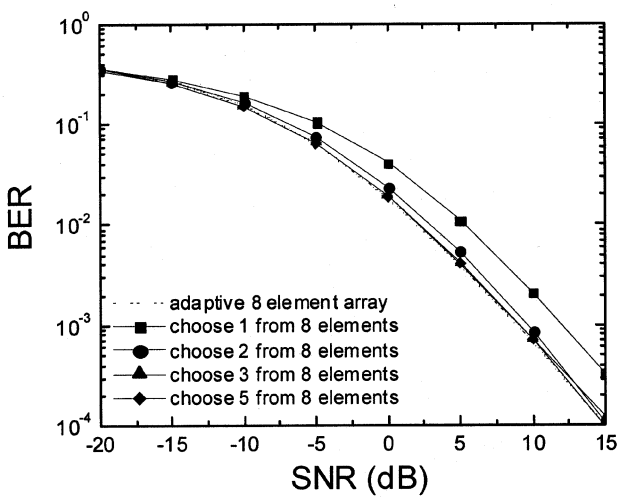

Fig. 13. Performance of a hybrid smart antenna system versus number of elements used by the optimum combining adaptive process. Simulation assumes no interference, and the number of signals was changed from one to five in an eight-element array. Simulations were performed for 120° beamwidth and 30° DOA spread.

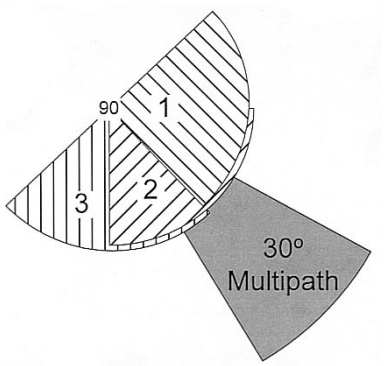

Fig. 14. Example of a 90° beamwidth system used in a 30° DOA spread environment.

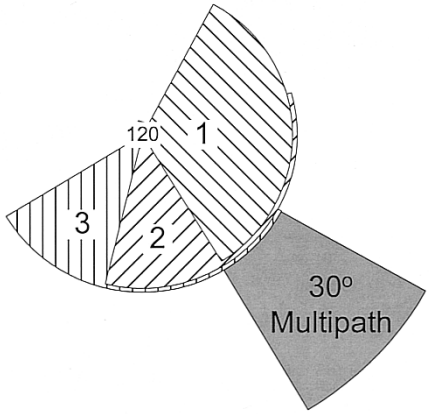

Fig. 15. Example of a 120° beamwidth system used in a 30° DOA spread environment.

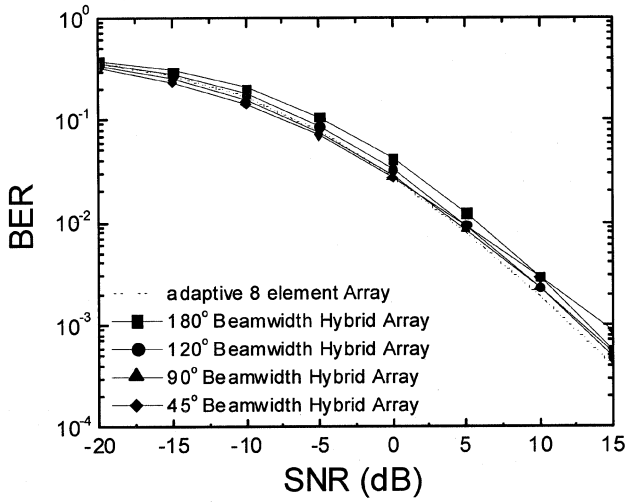

Fig. 16. Performance of hybrid smart antennas of directional elements with different beamwidths. Simulation assumes no interference, and that the hybrid array selects and combines two signals from an eight-element array of directional antennas. 10° DOA spread was also assumed.

signals with similar amplitude but different phases. Thus, a 90° beamwidth does not provide an optimum multipath combining system.

Fig. 15 shows a 120° beamwidth system used in the same 30° DOA spread environment. It is clear that, in this case, there is at least two antennas that can simultaneously receive all multipath signals within the assumed 30° DOA spread. Although a 120° beamwidth system has lower antenna gain, it achieves a higher optimum-combining gain and has a better composite gain than a 90° beamwidth system.

If the element pattern is too wide; however, the element gain will further decrease and the system performance will subsequently decrease. This clarifies the reduction in performance in the 180° beamwidth case shown in Fig. 12. Considering the fact that a hybrid smart antenna system only requires the number of signals to be as small as two (instead of eight signals) to achieve almost optimum performance, this presents a very encouraging observation and testifies to the significant performance improvement in the proposed hybrid system.

Figs. 16 and 17 show simulation results for a propagation model of five multipath signals with 10° DOA spread. It is a similar propagation scenario to that used in the simulation of Figs. 12 and 13, but the user is now at a relatively far distance from the base station and hence, the 10° DOA spread.

Fig. 16 shows how the beamwidth of each element in the array impacts the performance of the hybrid system. Fig. 17, on the other hand, illustrates the effect of the number of signals selected for optimum combining (NS) on the performance of the hybrid system. The results are similar to those shown in Figs. 12 and 13 in that the 120° beamwidth hybrid array provides the best performance, and that it is possible to select the number of signals (NS) to be as small as 2, in order to achieve improvement in the performance.

There is another common scenario in which multipath signals have a 360° DOA spread that may be of interest to simulate and analyze. This scenario corresponds to a broad distribution of DOA and may occur for the case of a base station in a typical Wireless Local Area Network (WLAN) and/or other indoor applications. In this kind of propagation environment, the base station is surrounded by walls, a ceiling, and furniture. All of which will cause multipath signals. Fig. 18 shows how different beamwidths impact the performance of a hybrid smart antenna system in a multipath environment with 360°

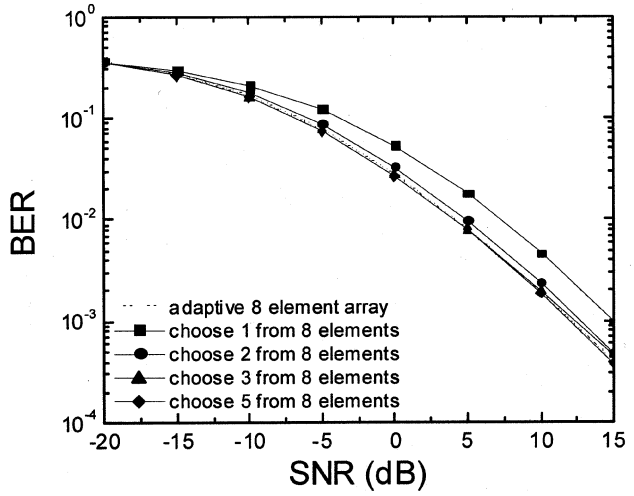

Fig. 17. Performance of hybrid smart antennas versus number of elements used by optimum combining. Simulation assumes no interference, and that the number of signals changes from one to five in an eight-element array of directional antennas. 120° beamwidth and 10° DOA spread were also assumed.

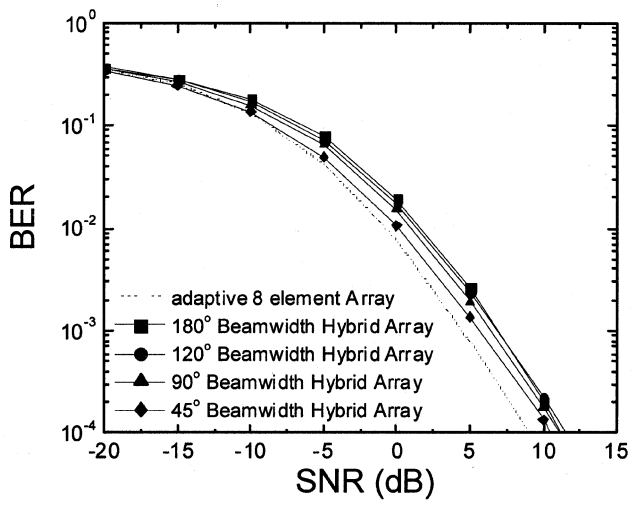

Fig. 18. Performance of hybrid smart antennas of directional elements with different beamwidths. Simulation assumes no interference, and that the hybrid array selects and combines two signals from an eight-element array of directional antennas. 360° DOA spread was also assumed.

DOA spread. As may be noted, the performance of a hybrid smart antenna that combines the two largest signals from eight elements gradually increases with the decrease in beamwidth. That is different from the situation in the 10 or 30° DOA spread multipath environments shown in Figs. 12 and 14. The reason for this is that the fading that occurs in each element is more independent in a 360° DOA spread environment. Thus the requirement that there should be some overlap among adjacent beam patterns in the 10° or 30° cases to achieve optimum combining is not valid in the 360° DOA case. In this case, (360° DOA) there is no optimum combining benefits that can be obtained by broadening the elements beam and hence sacrificing the gain. In a 360° DOA spread environment, higher antenna gain will provide better system performance. For example in a 45° beamwidth hybrid array, the required SNR to keep BER

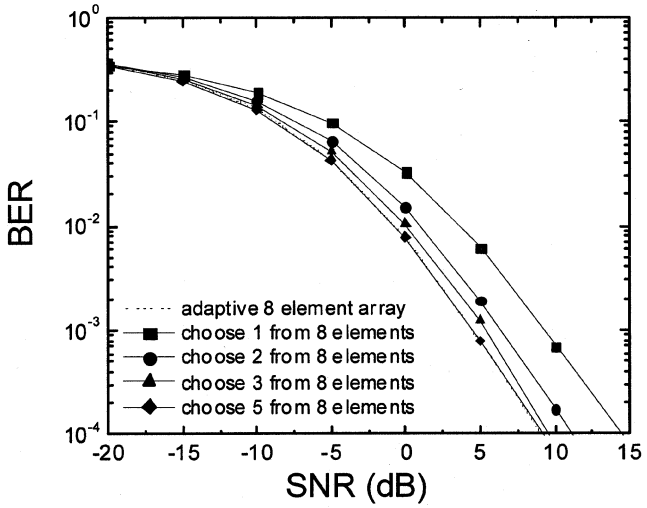

Fig. 19. Performance of hybrid smart antennas versus number of elements used by optimum combining. Simulation assumes no interference, and that the number of signals changes from one to five in an eight-element array of directional antennas. 90° beamwidth and 360° DOA spread were also assumed.

less than 10^{-3} is 1.1 dB higher than that for an adaptive smart antenna system. Based on these results, however, one may conclude that in a rich multipath environment, gains from narrower beamwidths are sufficiently small, and therefore, the use of omnidirectional antennas is not only justifiable but also suggested for practical consideration.

Fig. 19 shows how the number of signals chosen for optimum combining impact the performance of hybrid smart antennas in a 360° DOA spread environment. The beamwidth for each of the directional elements is chosen as 90°. The case of one chosen element is included to represent the traditional switched beam array. As shown in Fig. 19, to keep BER less than 10^{-3}, a switched-beam array requires a SNR 3 dB higher from that of two selected signals out of an eight-element array. When five signals were selected for optimum combining, results of the hybrid smart array superpose those from an adaptive array system.

Figs. 20 and 21 show simulation results for the case of spread-spectrum (CDMA) type systems. In this case, it is assumed that there are 20 users in the frequency band besides the desired user. All other users were uniformly distributed in the 360° range. The expected interference power from each cofrequency band user is 1/20 of that of the total noise. Since noise is normalized to one, the expected power of total interferences will, therefore, be 1, and this means that the expected interference to noise ratio is equal to 1. We also assumed five multipath signals and 30° multipath DOA spread.

Fig. 20 shows how the beamwidth of each element in the array impacts performance of the hybrid smart antenna system. It is similar to the simulation results presented earlier without interference. Once again beamwidth of radiating elements makes only a small impact on the overall performance. It may be noted that the 120° beamwidth of each element in the proposed hybrid smart antenna array would provide a slight improvement in performance over other simulated beamwidth values. To keep BER less than 10^{-3}, the proposed hybrid antenna needs a SNR 1.95 dB higher than the traditional adaptive smart antenna. This value, however, is higher than the 0.67 dB difference we obtained in the earlier simulations without interference. The dotted

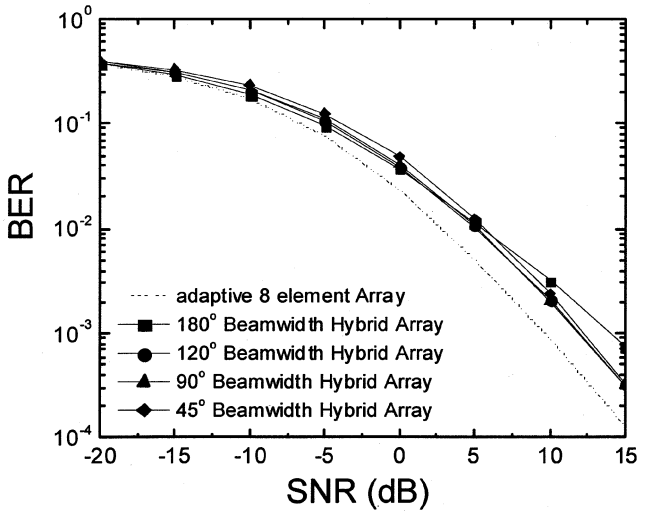

Fig. 20. Performance of hybrid smart antennas as a function of the beamwidth of the directional elements. Interference was included in this simulation, and the hybrid array was assumed to choose and combine two signals from an eight-directional element antenna array. A 30° DOA spread was also assumed.

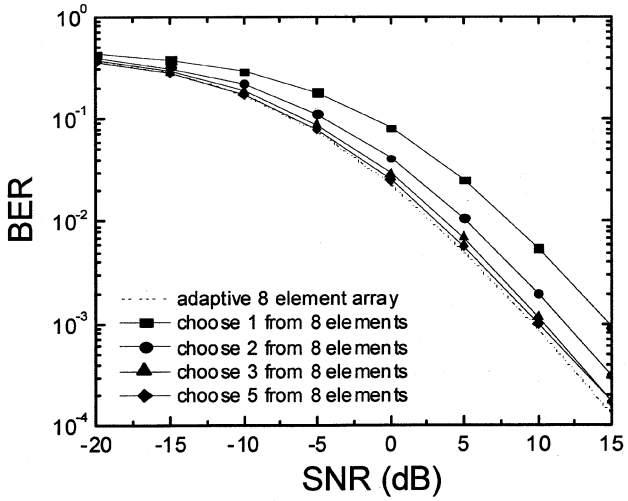

Fig. 21. Performance of hybrid smart antennas versus number of elements used by optimum combining. Interference was included in the simulation, and the hybrid array was assumed to choose one to five signals from eight directional elements. 120° beamwidth and 30° DOA spread were also assumed.

line in Fig. 20 is for the reference adaptive array. It may be also noted that with the proposed presence of interferences in the simulated CDMA system, the performance of the adaptive array was also degraded.

Fig. 21 shows the effect of the number of selected signals NS on the performance of the proposed hybrid smart antenna system. As shown in Fig. 21, three signals (instead of two as in earlier no-interference simulations) provide excellent combining results and the SNR needed to keep BER less than 10^{-3} is 0.7 dB higher than that for a traditional adaptive array.

V. Conclusion

In this paper we described a hybrid approach that integrates features of the switched beam smart antenna method with the beam forming approach of the adaptive antenna array technology. Unlike adaptive antenna array, the proposed method utilizes high gain antennas, and unlike the switched beam smart antenna approach, the proposed method performs a beam forming process on a smaller number of elements within the array. In the simulation results we assumed an antenna pattern that consists of one main lobe and a -20 dB side lobe arrangement. An eight-element antenna array was used throughout this study. Parameters studied include the beam width of the radiation pattern of the array elements, the number of multipath signals, the DOA spread, and the number of elements involved in the beam forming process. In all cases and even after the inclusion of interference signals, it is shown that the proposed hybrid process is more efficient as it utilizes a smaller number of signals (two to three instead of eight) in the beam forming process while providing BER values similar to those that can be achieved when using the entire eight signals in the adaptive array. The reduced number of elements also suggests reduced complexity and cost in performing the adaptive signal processing, and even possible improvement in performance as the adaptive process often involves a number of estimations. Specific analysis of the role of estimation on the performance of an adaptive antenna and the impact of a reduced number of estimations on the possible improvement in the accuracy and performance will be discussed in a separate article. Simulation results also showed a less significant impact of the antenna element beamwidth on the overall performance of the proposed hybrid system. For practical consideration, omnidirectional elements might as well be used. In this study we used the two or three largest signals from the eight-element array in the optimum-combining process. This may or may not be the best selection depending on the multipath environment. This aspect of the study needs further simulation that will be reported in a future article. Currently, on-going research efforts include taking into account the characteristics of the propagation environment, and the possible inclusion of parameters such as polarization diversity in evaluating the performance of the proposed hybrid antenna array system. Another area of research that is now being pursued is an experimental verification of some of the reported observations by combining the outputs of a set of omni-directional antennas using a Butler matrix. This idea was proposed by one of the reviewers. The most important outcome from the present study; however, is related to the possible use of a smaller number of signals in the optimum-combining adaptive process while maintaining a performance similar to that of a fully adaptive, and, hence, more complex approach.

Acknowledgment

The authors wish to acknowledge the constructive comments and suggestion provided by the reviewers. Their kind effort certainly contributed to the quality of this publication.

References

[1] S. Bellofiore *et al.*, "Smart antenna system analysis, integration and performance for Mobile Ad-Hoc Networks (MANET's)," *IEEE Trans. Antennas Propagat.*, vol. 50, pp. 571–581, May 2002.

[2] M. Ho, G. Stuber, and M. Austin, "Performance of switched-beam smart antennas for cellular radio systems," *IEEE Trans. Vehic. Technol.*, vol. 47, pp. 10–19, Feb. 1998.

[3] R. C. Bernhardt, "The use of multiple-beam directional antennas in wireless messaging systems," in *Proc. IEEE Vehicular Technology Conf.*, 1995, pp. 858–861.

[4] A. F. Naguib, A. Paulraj, and T. Kailath, "Capacity improvement with BS antenna arrays in cellular CDMA," *IEEE Trans. Vehic. Technol.*, vol. 43, pp. 691–698, Aug. 1994.

[5] P. Strobach, "Total least squares phased averaging and 3-D ESPRIT for joint azimuth-elevation-carrier estimation," *IEEE Trans. Signal Processing*, vol. 49, pp. 54–62, Jan. 2001.
[6] B. Widrow and S. D. Stearns, *Adaptive Signal Processing*. Englewood Cliffs, NJ: Prentice-Hall, 1985.
[7] J. C. Liberti Jr. and T. S. Rappaport, *Smart Antennas for Wireless Communications: IS-95 and Third Generation CDMA Applications*. Upper Saddle River, NJ: Prentice-Hall, 1981, 1999.
[8] J. Foutz and A. Spanias, "Adaptive modeling and control of smart antenna arrays," in *Proc. IASTED Int. Conf. Modeling, Identification. Contr.—MIC 2001*, Innsbruck, Austria, Feb. 2001.
[9] P. Darwood, P. N. Fletcher, and G. S. Hilton, "Mutual coupling compensation in small planar array antennas," in *Proc. IEE Microwaves, Antennas and Propagation*, vol. 145, Feb. 1998, p. .
[10] J. H. Winters, "Signal acquisition and tracking with adaptive arrays in the digital mobile radio system IS-54 with flat fading," *IEEE Trans. Vehic. Technol.*, vol. 42, pp. 377–384, Nov. 1993.
[11] H. Matsuoka, Y. Murakami, H. Shoki, and Y. Suzuki, "A smart antenna receiver testbed with directional antenna elements," in *IEEE Int. Conf. Phased Array Syst. Technol.*, 2000, pp. 113–116.
[12] M. Win and J. H. Winters, "Virtual branch analysis of symbol error probability for hybrid selection/maximal-ratio combining in Rayleigh fading," *IEEE Trans. Commun.*, vol. 49, pp. 1926–1934, Nov. 2001.
[13] P. Petrus, J. Reed, and T. Rappaport, "Geometrical-based statistical macrocell channel model for mobile environments," *IEEE Trans. Communicat.*, vol. 50, pp. 495–502, Mar. 2002.
[14] J. Liberti and T. Rappaport, "A geometrically based model for line-of-sight multipath radio channels," in *IEEE Vehic. Technol. Conf.*, vol. 2, 1996, pp. 844–848.
[15] E. Villier, "Performance analysis of optimum combining with multiple interferers in flat Rayleigh fading," *IEEE Trans. Commun.*, vol. 47, pp. 1503–1510, Oct. 1999.

Zhijun Zhang (M'00) received the B.S. and M.S. degrees in electrical engineering from the University of Electronic Science and Technology of China, Chengdu, in 1992 and 1995, respectively, and the Ph.D. degree in electrical engineering from Tsinghua University, Beijing, China, in 1999.

From 1999 to 2001, he was a Postdoctoral Fellow with the Department of Electrical Engineering, University of Utah. He was appointed a Research Assistant Professor in same the Department in 2001. He was with the University of Hawaii in 2002, where he was an Assistant Researcher. He joined Amphenol Mobile in 2002, where he is currently a Senior Staff Antenna Development Engineer.

Magdy F. Iskander (F'93) is the Director of the Hawaii Center for Advanced Communications (HCAC), College of Engineering, University of Hawaii at Manoa, Honolulu. He was a Professor of Electrical Engineering and the Engineering Clinic Endowed Chair Professor at the University of Utah for 25 years. He was also the Director of the Center of Excellence for Multimedia Education and Technology. From 1997 to 1999, he was a Program Director, in the Electrical and Communication Systems Division of the National Science Foundation (NSF). At NSF, he formulated and directed a "Wireless Information Technology" initiative in the Engineering Directorate and funded over 29 projects in the microwave/millimeter wave devices, RF MEMS technology, propagation modeling, and the antennas areas. He edited the special issue of the IEEE TRANSACTIONS ON ANTENNAS AND PROPAGATION, May 2002, which included contributions from the NSF funded projects. In 1986, he established the Engineering Clinic Program to attract industrial support for projects for undergraduate engineering students and has been the Director of this program since its inception. To date, the program has attracted more than 115 projects sponsored by 37 corporations from across the US. The Clinic Program now has an endowment for scholarships and a professorial chair held by the Director at the University of Utah. He spent sabbatical and other short leaves at Polytechnic University of New York; Ecole Superieure D'Electricite, France; UCLA; Harvey Mudd College; Tokyo Institute of Technology; Polytechnic University of Catalunya, Spain; and at several universities in China. He has published over 170 papers in technical journals, has nine patents, and has made numerous presentations in technical conferences. He authored a textbook on *Electromagnetic Fields and Waves* (Englewood Cliffs, NJ: Prentice-Hall: 1992); edited the *CAEME Software Books* (Vol. I, 1991, and Vol. II, 1994); and edited four other books on *Microwave Processing of Materials*, (Materials Research Society, 1990–1996). He edited four special issues of Journals including two for the *Journal of Microwave Power*, and a special issue of the *ACES Journal*. He also edited the 1995 and 1996 proceedings of the *International Conference on Simulation and Multimedia in Engineering Education*. He is founding editor of the journal, *Computer Applications in Engineering Education* (CAE), (Wiley), which received the Excellence in Publishing award in 1993. His ongoing research contracts include "Propagation Models for Wireless Communication," funded by the Army Research Office and NSF; "Low-Cost Phased Array Antennas," funded by both the Army Research Lab and NSF; "Electronically tunable microwave devices," funded by Raytheon, "Microwave Processing of Materials," funded by Corning, Incorporated; and the "Conceptual Learning of Engineering" project funded by NSF.

Dr. Iskander received the 1985 Curtis W. McGraw ASEE National Research Award, 1991 ASEE George Westinghouse National Education Award, 1992 Richard R. Stoddard Award from the IEEE EMC Society, and the 2000 University of Utah Distinguished Teaching Award. He was a member of the WTEC panel on "Wireless Information Technology," and the Chair of the Panel on "Asia Telecommunications" sponsored by DoD and organized by the International Technology Research Institute (ITRI) in 2000–2001. As part of these studies, he visited many wireless companies in Europe, Japan, and several telecommunications institutions and companies in Taiwan, Hong Kong, and China. He was a member of the National Research Council Committee on Microwave Processing of Materials. He organized the first "Wireless Grantees Workshop" sponsored by NSF and held at the National Academy of Sciences, in 2001. He was the 2002 President of the IEEE Antennas and Propagation Society, the Vice President in 2001, and was a member of the IEEE APS AdCom from1997 to 1999. He was the General Chair of the 2000 IEEE AP-S Symposium and URSI meeting in Salt Lake City, UT, and was a Distinguished Lecturer for the IEEE AP-S (1994–1997). While serving as a distinguished lecturer of the IEEE, he has given lectures in Brazil, France, Spain, China, Japan, and at a large number of U.S. universities and IEEE chapters.

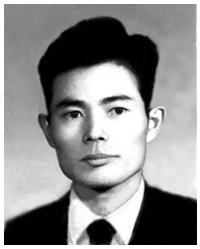

Zhengqing Yun (M'98) received the Ph.D. degree in electrical engineering from Chongqing University, Chongqing, China, in 1994.

He was a Postdoctoral fellow from 1995 to 1997 with the State Key Laboratory of Millimeter Waves, Southeast University, Nanjing, China. From 1997 to 2002, he was with the Electrical Engineering Department, University of Utah. He is currently an Assistant Researcher with the Hawaii Center for Advanced Communication, University of Hawaii, Manoa. His recent research interests include development of numerical methods, modeling of radio propagation for wireless communications systems including MIMO, and design and simulation of antennas.

Dr. Yun was the recipient of the 1997 Science and Technology Progress Award (1st Class) presented by The State Education Commission of China.

Anders Høst-Madsen (M'95–SM'02) was born in Denmark in 1966. He received the M.Sc. degree in electrical engineering in 1990 and the Ph.D. degree in mathematics in 1993, both from the Technical University of Denmark.

From 1993 to 1996 he was with Dantec Measurement Technology A/S, Denmark, from 1996 to 1998 he was an Assistant Professor with the Kwangju Institute of Science and Technology, Korea, and from 1998 to 2000, he was an Assistant Professor with the Department of Electrical and Computer Engineering, University of Calgary, Canada, and a staff scientist at TR Labs, Calgary. In 2001 he joined the Department of Electrical Engineering, University of Hawaii, as an Assistant Professor. He has also been a visitor with the Department of Mathematics, University of California, Berkeley, through 1992. His research interests are in statistical signal processing and wireless communications, including multiuser detection, equalization, and *ad hoc* networks.